Structure−Function Engineering of Interferon-β-1b for Improving Stability, Solubility, Potency, Immunogenicity, and Pharmacokinetic Properties by Site-Selective Mono-PEGylation

Amartya Basu, Karen Yang, Maoliang Wang, Sam Liu, Ramesh Chintala, Thomas Palm, Hong Zhao, Ping Peng, Dechun Wu, Zhenfan Zhang, Jack Hua, Ming-Ching Hsieh, John Zhou, Gerald Petti, Xiguang Li, Ahsen Janjua, Magda Mendez, Jun Liu, Clifford Longley, Zhihua Zhang, Mary Mehlig, Virna Borowski, Manickam Viswanathan, and David Filpula*

Enzon Pharmaceuticals, 20 Kingsbridge Road, Piscataway, New Jersey 08854-3969. Received November 9, 2005; Revised Manuscript Received February 22, 2006

Recombinant interferon-beta-1b (IFN-β-1b) is used clinically in the treatment of multiple sclerosis. In common with many biological ligands, IFN-β-1b exhibits a relatively short serum half-life, and bioavailability may be further diminished by neutralizing antibodies. While PEGylation is an approach commonly employed to increase the blood residency time of protein therapeutics, there is a further requisite for molecular engineering approaches to also address the stability, solubility, aggregation, immunogenicity and in vivo exposure of therapeutic proteins. We investigated these five parameters of recombinant human IFN-β-1b in over 20 site-selective mono-PEGylated or multi-PEGylated IFN-β-1b bioconjugates. Primary amines were modified by single or multiple attachments of poly(ethylene glycol), either site-specifically at the N-terminus, or randomly on the 11 lysines. In two alternate approaches, site-directed mutagenesis was independently employed in the construction of designed IFN-β-1b variants containing either a single free cysteine or lysine for site-specific PEGylation. Optimization of conjugate preparation with 12 kDa, 20 kDa, 30 kDa, and 40 kDa amine-selective PEG polymers was achieved, and a comparison of the structural and functional properties of the IFN-β-1b proteins and their PEGylated counterparts was conducted. Peptide mapping and MALDI-TOF mass spectrometric analysis confirmed the attachment sites of the PEG polymer. Independent biochemical and bioactivity analyses, including antiviral and antiproliferation bioassays, circular dichroism, capillary electrophoresis, flow cytometric profiling, reversed phase and size exclusion HPLC, and immunoassays demonstrated that the functional activities of the designed IFN-β-1b conjugates were maintained, while the formation of soluble or insoluble aggregates of IFN-β-1b was ameliorated. Immunogenicity and pharmacokinetic studies of selected PEGylated IFN-β-1b compounds in mice and rats demonstrated both diminished IgG responses, and over 100-fold expanded AUC exposure relative to the unmodified protein. The results demonstrate the capacity of this macromolecular engineering strategy to address both pharmacological and formulation challenges for a highly hydrophobic, aggregation-prone protein. The properties of a lead mono-PEGylated candidate, 40 kDa PEG_2−IFN-β-1b, were further investigated in formulation optimization and biological studies.

INTRODUCTION

Human interferon-beta (IFN-β[1]) is produced in many cell types in response to viral infection or exposure to double stranded RNA (*1*, *2*). Following binding of this glycoprotein to a heterodimeric cell receptor, IFNAR-1/IFNAR-2, a cascade of signaling events leads to expression of IFN-β inducible genes which modulate antiviral, antiproliferative, and immunomodulatory functions (*3*−*6*). Three recombinant IFN-β therapeutics are presently marketed for the treatment of the relapsing-remitting form of multiple sclerosis (*7*−*12*). IFN-β-1a preparations are glycosylated products expressed in mammalian cells and are similar to the 166 amino acid native human protein. IFN-β-1b is a nonglycosylated protein expressed in *E. coli*; it also differs from the human protein in that it lacks the N-terminal methionine and has a Cys17Ser substitution (*13*−16). These structural alterations may correlate with an apparent reduced bioactivity in vitro and an increase in neutralizing antibodies for patients treated with IFN-β-1b when compared with IFN-β-1a (*17*−*22*). While both of the Type I interferons, IFN-α and IFN-β, which bind to a common IFNAR-1/IFNAR-2 receptor (*23*−*25*), have proven to be among the most successful biotechnology products, the major obstacle to clinical development has not been biological potency. Rather, the physicochemical properties of these very potent compounds have led to challenges in frequent dosing, formulation, and immunogenicity. Among the human therapeutic cytokines, IFN-β-1b is a prime example of a hydrophobic protein difficult to purify and formulate, owing to the propensity of the molecule to form aggregates. The marketed IFN-β-1b product, Betaseron, is a lyophilized powder containing human serum albumin as an excipient. Clinical pharmacokinetic studies have demonstrated that IFN-β-1b has a very short terminal serum half-life and the

* To whom correspondence should be addressed. Tel: 732-980-4941. Fax: 732-885-2950. E-mail: david.filpula@enzon.com.

[1] Abbreviations: ALD, aldehyde; AUC, area under the curve; ELISA, enzyme-linked immunosorbent assay; HAc, acetic acid; HRP, horseradish peroxidase; HSA, human serum albumin; IFN-β-1b, interferon beta-1b; im, intramuscular; iv, intravenous; mAb, monoclonal antibody; mPEG, monomethoxy-PEG; MRT, mean retention time; MW, molecular weight; NHS, *N*-hydroxysuccinimide; PBS, phosphate-buffered saline; PEG, poly(ethylene glycol); PEG_2, branched PEG; RP, reversed phase; sc, subcutaneous; SC, succinimidyl carbonate; SE-HPLC, size-exclusion-high performance liquid chromatography; SPA, succinimidyl propionate; $t_{1/2}$, serum half-life; TFA, trifluoroacetic acid; T-PEG, thiazolidine-2-thione PEG; U-PEG, branched PEG; X-US-PEG, extended branched PEG.

10.1021/bc050322y CCC: $33.50
Published on Web 05/03/2006

low serum concentrations challenge the limits of assay detection following subcutaneous administration (*14*, *26*).

The goals of the present study were to design IFN-β-1b molecules exhibiting (1) prolonged solubility in the absence of detergents, (2) diminished formation of protein aggregates, (3) diminished immunogenicity, (4) improved in vivo potency, and (5) tailored pharmacokinetic profiles with alternate routes of administration. We wished to employ bioconjugate and protein engineering approaches to investigate the performance of a series of designed IFN-β-1b compounds synthesized by site-specific or site-selective surface modification. PEGylation, the covalent attachment of poly(ethylene glycol) polymers to compounds, has become one of the best validated drug delivery methods for extension of serum half-life (*27*−*38*) and at least six PEGylated protein therapeutics are now on the market (*39*). Two PEGylated interferon-α products are included in this category (*40*−*45*) and initial progress on PEG−IFN-β-1a has been reported (*34*, *46*, *47*), but a general strategy for creating tailored PEGylated IFN-β-1b has not been developed after the1990 patent disclosure of Katre and Knauf (*48*). Conjugates composed of PEG and receptor-binding ligands frequently exhibit diminution or even loss of bioactivity, and these compounds may also demonstrate substantial product heterogeneity. In general, activated PEG polymers reactive with primary amines have been employed in multiple attachments with catabolic enzymes and other macromolecules which recognize small substrates. In comparison, PEGylation of cytokines, hormones, and other small protein ligands represents a greater challenge for enhancing clinical potency due to the opposing effects of reduced receptor binding affinity and prolonged conjugate circulating lives (*49*−*52*). A receptor binding site may constitute a large proportion of the ligand surface area; for example, 960 Å^2 of accessible surface is buried in each binding interface of the IFN-γ/IFN-γRα complex (*53*). Furthermore, reactive amines are prevalent moieties on the scaffold and contact regions of essentially all natural cytokine sequences (*2*). Consequently, extensive random conjugations may be inactivating either through direct attachment to receptor-binding contact residues or as a result of transient steric hindrance and diffusional constraints from the long polymer strands.

To investigate this macromolecular engineering approach, we expressed purified and re-engineered recombinant IFN-β-1b through construction of 20 disparate conjugate preparations with 12 kDa, 20 kDa, 30 kDa, and 40 kDa PEG polymers and performed a comparison of the structural and functional properties of the purified IFN-β-1b proteins and their PEGylated counterparts. Physicochemical analysis of selected mono-PEGylated IFN-β-1b compounds verified their composition, while several cell based assays, immunoassays, and chromatographic methods confirmed that the conjugates demonstrated superior monomeric stability and maintained functional activity dependent on microenvironment. Pharmacokinetic studies of the conjugates in rodents demonstrated that the circulating lives of the PEGylated IFN-β-1b proteins could be tailored with correspondence to the polymer molecular mass, reaching circulating times comparable to the major blood proteins for the conjugate compounds employing 40 kDa branched PEG polymers. These investigations demonstrate a practical approach for engineering IFN-β-1b, and perhaps other similar hydrophobic proteins, to achieve improved physical stability as well as improved pharmacological properties.

EXPERIMENTAL PROCEDURES

Materials. Recombinant human IFN-β-1b (30 MIU/mg) was supplied by Enzon Pharmaceuticals (Piscataway, NJ). Betaseron was purchased from the pharmacy. All activated PEG polymers were supplied by Enzon Pharmaceuticals, except mPEG2-ButyrALD-40 kDa-PEG, mPEG-SPA-20 kDa and mPEG2-NHS-40 kDa, which were purchased from Nektar Therapeutics (San Carlos, CA). Hiload Superdex 200, HiPrep 26/10, and PD-10 desalting columns were supplied by Amersham BioSciences (now GE Healthcare, Piscataway, NJ), and Poros HS was supplied by Applied Biosystems (Foster City, CA). Precast 4−20% Tris-glycine SDS PAGE gels and the gel running buffer were obtained from Invitrogen (Carlsbad, CA). Encephalomyocarditis virus (EMCV; VR-129B) and Vero cells (CCL-81) were from ATCC. Titrisol iodine solution was obtained from EM Science (Gibbstown, NJ).

IFN-β-1b Genetic Constructions. The synthetic genes for human IFN-β-1b and protein variants were constructed from the published sequence (*13*). Recombinant proteins were expressed in *E. coli* BL21(DE3), refolded, and purified to near homogeneity as previously described (*54*, *55*). The inclusion of 0.05% Zwittergent 3−14 in column and formulation buffers was needed to maintain protein solubility. DNA sequence confirmation of all IFN-β genes was performed on an ABI PRISM 310 Genetic Analyzer. Generation of lysine-free variants of IFN-β-1b followed the reported protocol (*52*).

PEGylation of IFN-β-1b. IFN-β-1b (0.8 mg/mL; 5−50 mL) in 100 mM sodium phosphate, 0.05% Zwittergent 3−14, 2 mM EDTA, pH 7.8, was conjugated with activated PEG polymers with PEG mass of 12 kDa, 20 kDa, 30 kDa, and 40 kDa. In random PEGylation of primary amines, PEG-NHS or PEG-T compounds were dissolved in 0.1 mM HAc (or in H_2O for T-PEG). With fast stirring without generating foam, the PEG solution was added at 0.5−1.0 g/min to a final 10-fold molar excess over protein. The reaction was conducted at 25 °C for 60 min for PEG-NHS, or 120 min for PEG-T, quenched by adding glycine to a final molar ratio of 50:1 (glycine:PEG), and filtered through a 0.2 μm membrane before the column purification.

N-Terminal PEGylation: IFN-β-1b (0.8 mg/mL) was reacted with ALD-PEG polymers at a 1:10 reaction molar ratio in 100 mM sodium acetate, pH 5.2, at 25 °C for 3 h. 1 M sodium cyanoborohydride in PEGylation buffer was added to the reaction to a final concentration of 15 mM. The reaction was conducted at 25 °C for 16 h.

Purification of PEG−IFN-β-1b. The PEGylation reaction (5 mL; 0.8 mg protein/mL) was purified by Superdex 200 High Load chromatography with a 10 mM sodium phosphate, pH 7.3, 0.05% Zwittergent running buffer at a flow rate of 2 mL/min. In the second step, 8 mL of peak fractions were loaded onto an HS-50 column with 10 mM sodium phosphate, pH 7.3, 5% mannitol running buffer. The PEG−IFN-β-1b was eluted with 1 M NaCl in equilibration buffer at 2 mL/min and 2 mL/fraction over a period of 40 min. Fractions identified on SDS−PAGE were combined and the pH of the sample was immediately adjusted to 3.7 with HAc. It was then dialyzed using a 30k-MW-cutoff membrane against 5% mannitol, 3 mM HAc, pH 3.7 at 4 °C for 12 h. The fractions were diafiltered on Amicon membranes to a final concentration of 0.5−1 mg/mL in 3 mM HAc, pH 3.7, 5% mannitol. The endotoxin levels of the IFN-β-1b conjugates were <1 EU/mg; contamination of *E. coli* proteins was below 0.002% by immunoassay (Cygnus Technologies); Zwittergent and SDS were undetectable by RP-HPLC using an ELSD detector (detection limit: 0.01%) and acridine-orange (detection limit: 0.001%), respectively.

Analytical Characterization of IFN-β-1b and PEG−IFN-β-1b. Protein concentrations were determined by UV absorbance at 280 nm, with an IFN-β-1b extinction coefficient of 1.5 mL/mg.cm. The concentration was also confirmed by the bicinchoninic acid assay (BCA) using a BSA standard.

Western blot analysis was performed with anti-huIFN-β rabbit antiserum as a primary antibody and goat anti-rabbit HRP was

used as a secondary antibody with a TMBM peroxidase substrate. Iodine staining of SDS PAGE gels was performed after gels were rinsed with distilled water and placed in 5% barium chloride solution. After 10 min of gentle mixing, the gels were again rinsed with water and placed in 0.1 M Titrisol iodine solution for color development.

Mass values of IFN-β-1b and PEG−IFN-β-1b conjugates were determined by matrix-assisted laser desorption ionization−time-of-flight mass spectrometry (MALDI-TOF; Bruker Daltronics OmniFlex NT) using an internal standard with similar molecular weight on the α-cyano-4-hydroxycinnamic acid (CHCA) matrix. Apparent molecular weights (Stoke radius) of the compounds were estimated using Superdex 200 HR 10/30 Gel Filtration column chromatography. Additionally, analysis of molecular masses on 4−20% SDS−PAGE gels was performed using protein and PEG-protein standards.

Peptide mapping was performed by published procedures (*57*).The PEG−IFN-β-1b (0.2 mg) was denatured and reduced in 6 M guanidine HCl, 1 mM EDTA, 5 mM DTT, then alkylated with iodoacetamide prior to digestion with TPCK-treated trypsin. The trypsin generated peptide mixture was fractionated by size exclusion chromatography (Superdex 75) with HPLC-grade water and analyzed by SDS−PAGE and iodine staining. The unique iodine-stained fraction was subjected to protein sequencing analysis (PROCISE, Applied Biosystems). Alternatively, the PEG-peptide fragments were isolated on RP-HPLC and subsequently subjected to sequencing. The percent isomer was calculated by dividing the amount of each isomer by the total amount of isomers in the first cycle of sequencing. Lys-C digested fragments from either IFN-β-1b or PEG−IFN-β-1b were also separated on RP-HPLC and identified by LC-MS. PEG-peptides were identified by comparative analysis.

Circular dichroism (CD) and the determination of enthalpy of folding were conducted as described (*58*). All samples were analyzed at 0.1 mg/mL in 5 mM acetic acid. Spectra were collected at 25 °C. Data were analyzed using the neural network software CDNN (*59*).

Flow cytometry for comparative analysis of fluorescence intensity was conducted on FACSCalibur as previously described (*28*). A549 cells were incubated sequentially with IFN-β-1b, rat anti IFN-β-1b or anti PEG−IFN-β-1b plasma, and PE conjugated goat anti- rat IgG polyclonal antibody (BD Biosciences).

Biacore analysis was performed as described (*28*). IFN-β-1b was immobilized on a CM5 chip and the preimmunized and postimmunized rat serum (1:100) were analyzed for antibodies against IFN-β-1b.

RP-HPLC. RP-HPLC was used to determine conjugate purity and stability. A Vydac C4 column was run at 55 °C. Samples (0.5 mg/mL in 5% mannitol, 3 mM HAc, pH 3.7) were analyzed using a 45−60% gradient over 25 min at 0.8 mL/min of buffer A (0.1% TFA in H_2O) and buffer B (0.1% TFA in acetonitrile).

SE-HPLC. Superdex 200 HR was used to analyze formation of soluble aggregates of the PEG−IFN-β conjugates. The mobile phase was composed of 100 mM sodium phosphate, pH 6.8, at 24 °C. Evaporative Light Scattering Detection (ELSD; Sedere, Inc.) allowed free PEG detection.

Antiviral Assays of IFN-β-1b. Specific antiviral activity from the cytopathic effect of IFN-β-1b was assayed by published methods (*60*) using Vero cells and EMCV virus, which were cultivated as recommended by the ATCC supplier. Vero cells were distributed on 96-well microtiter plates (20000 cells/well) in 0.05 mL of culture medium. Serial dilutions of 0.05 mL of the IFN-β samples were added and incubated at 37 °C, 5% CO_2, for 24 h. EMCV (200 pfu/20 μL) was added to each well at 25 °C for 30 min and then incubated at 37 °C for 24 h. After the addition of 20 μL of 10 mg/mL 3-(4,5-dimethyl-2-thiazoyl)-2,5-diphenyl-2*H*-tetrazolium bromide (MTT; Promega, Madison, WI) dye solution to each well, incubation was continued for 4 h; then 100 μL of stop solution (1.2 N HCl in 2-propanol) was added to each well, and the plate was read at 570 nm in a 96-well plate reader (Molecular Devices, Sunnyvale, CA) to determine EC_{50} values, as analyzed with Softmax Pro software. Native IFN-β-1b and PEGylated IFN-β-1b were analyzed in triplicate on each plate. Conversion of mass to antiviral units was attained using specific activity of the parent compound (native or PEG−IFN-β-1b). A549 cells were also used in antiviral assays in this procedure.

Antiproliferation Assay. A549 cells were seeded in 96-well plates, 4000 cells/well, in 100 μL complete Ham's F12K medium containing 2 mM L-glutamine, 1.5 g/L sodium bicarbonate, and 10% fetal bovine serum. IFN-β-1b compounds were added to the cells (in triplicate) in serial dilutions, initiating at 125 ng/mL, which is equivalent to 4000 Units/mL of Betaseron activity. Cells were allowed to grow for 4 days, and cell proliferation was measured by the MTT assay.

Pharmacokinetic Analysis of PEG−IFN-β-1b in Mice. C57BL/6 mice (7−8 week, female) were supplied by Sprague Dawley Harlan (Madison, WI). Mice (5/group) were injected subcutaneously, intramuscularly, and intravenously with 100 μL per mouse (0.2 mg protein/kg) of IFN-β-1b, or its PEGylated conjugates. Following sedation with 0.09% avertin, sampling of blood was undertaken via the retro-orbital sinus into vials containing EDTA. At 2, 15, 30, and 60 min, the mice were bled 100 μL, and at 4, 24, 48, 72, and 96 h, the mice were terminally bled by cardiac puncture. The plasma was collected following centrifugation of the blood at 5000 rpm at 4 °C for 5 min and immediately frozen on dry ice. The concentrations of the compounds were analyzed by both antiviral activity and by ELISA. The data were modeled using WinNonlin software (WinNonlin Pharsight, Mountain View, CA) to determine pharmacokinetic parameters using a two compartment, bolus, first-order elimination model for the intravenous samples. The correlation between the observed and predicted model time point values was ≥95%.

Pharmacokinetic Analysis of PEG−IFN-β-1b in Rats. Sprague Dawley (Harlan) rats (150−300 g; 3/group) were injected subcutaneously, intramuscularly, or intravenously with 150 μL per rat (0.1−0.6 mg/kg) of IFN-β-1b, or its PEGylated conjugates. Following sedation with 30% O_2/70% CO_2, sampling of blood (250 μL) was undertaken via the retro-orbital plexus into vials containing EDTA, at times prior to compound administration and at 2 min, 60 min, 2 h, 4 h, 8 h, 24 h, and daily for 3 additional days. The plasma was collected following centrifugation of the blood at 5000 rpm at 4 °C for 5 min and immediately frozen on dry ice. The concentrations of the compounds were analyzed by both antiviral activity and by ELISA. The data were modeled using WinNonlin software (WinNonlin Pharsight, Mountain View, CA) by noncompartmental analysis with AUC estimated by the linear trapezoidal rule to determine pharmacokinetic parameters.

Immunogenicity of IFN-β-1b and PEG−IFN-β-1b in Rats. Sprague Dawley (Harlan) rats weighing 150−300 g (three in a group) were injected intramuscularly with either buffer, native IFN-β-1b (0.1 mg/kg), or NHS 40 kDa PEG_2−IFN-β-1b (0.1 mg protein/kg). Injections were given once per week for five weeks, and the plasma samples were collected before the next injection and at the end of the sixth week. Rat plasma antibodies were analyzed by direct ELISA, indirect ELISA, flow cytometry, Biacore, and antiviral neutralization assays.

Direct ELISA: As previously described (*61*), IFN-β-1b coated the microtiter plates (400 ng/50 μL). Rat anti IFN-β-1b or anti PEG−IFN-β-1b plasma was added in 1:2 serial dilutions. The secondary antibody was HRP conjugated rabbit anti rat IgG

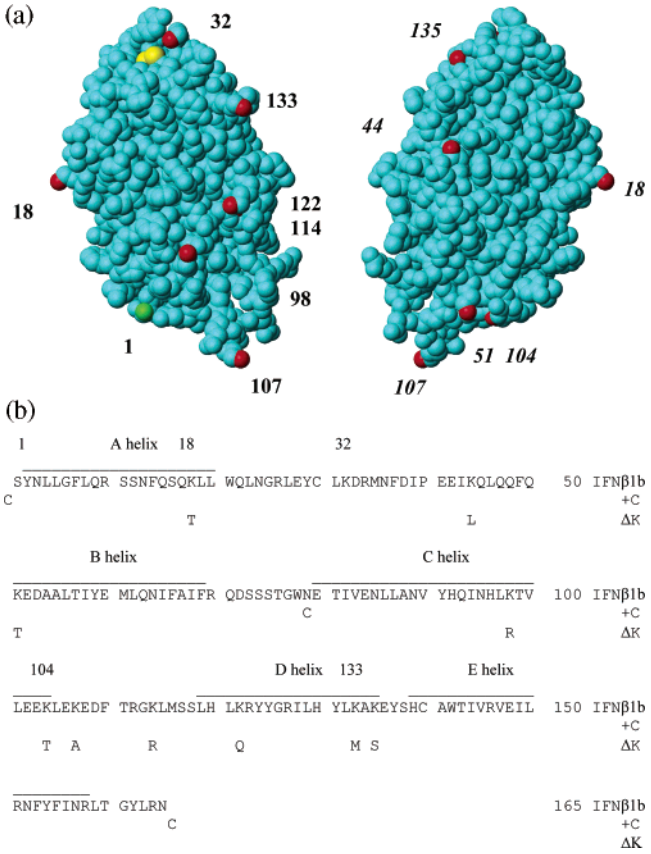

Figure 1. (A) Two views of the human IFN-β model based on the IFN-β-1a crystal structure (PDB File Name 1AU1). The space-filling model is shown from two different angles, rotated by 180°. The 11 lysines are numbered and highlighted with nitrogen in red. The right-hand model uses italics numbering for clarity. The N-terminal serine-1 amino group is green and the disulfide (S−S) bond between cysteine-30 and cysteine-140 is shown in yellow. Lysine-114 is not readily visible in this figure. (B) Amino acid sequence of 165-residue IFN-β-1b is shown with five helix structures. Locations of primary sites of PEGylation at lysines or the N-terminus are shown by numbering above the sequence. Below the sequence are shown site-specific mutant proteins corresponding to sites of single free cysteine insertion (+C) at either the N-terminus, C-terminus, or position 79. Also shown on the bottom line are the sequence substitutions in a lysine depleted variant protein (ΔK).

(Jackson Labs; 1:5000) with TMB peroxidase substrate (Moss, Inc.). Plates were read at 450 nm. The control mAb MMHB-3 was obtained from R&D Systems.

Indirect ELISA: The microtiter plates were coated with the capture antibody, anti- huIFN-β mAb (R&D Systems) at 200 ng/50 μL per well. After blocking, either 4 ng or 20 ng of the two test compounds, IFN-β-1b and NHS 40 kDa PEG_2−IFN-β-1b, were added in alternate wells and incubated 12 h at 4 °C. After washing, rat plasma samples were added in 1:2 serial dilutions, beginning at 1:100 or 1:1000 dilutions for IFN-β-1b or NHS 40 kDa PEG_2−IFN-β-1b, respectively. After 12 h incubation at 4 °C and plate washing with PBS, 0.05% Tween-20, pH 7.4, 50 μL of HRP conjugated goat anti rat IgG (1:5000; Jackson Labs) was added and after 2 h incubation at 22 °C and plate washing, TMBE−100 substrate (Moss, Inc.) was incubated for 20 min and the plates were read at 450 nm.

RESULTS AND DISCUSSION

Recombinant Human IFN-β-1b and Site-Selective PEGylation Strategy. A structural view of IFN-β-1b architecture is shown in Figure 1A and 1B (*13, 15*). In our investigations of PEGylation of this protein, we wished to examine multiple approaches which would include attachment of PEG polymers at several different positions on the protein surface. Other investigated parameters would include PEG size, PEG linker, and number of polymer attachments per protein. The key characteristics under evaluation for improved performance would include blood residency time, potency, solubility, aggregation, and immunogenicity. To minimize the potential for PEG polymer strands to sterically block the receptor-binding sites, our preferred designs place single attachments of PEG either (1) site-specifically at the N-terminus, (2) site-selectively on lysines in a stochastic mixture of mono-PEGylated products, or (3) site-specifically in engineered attachment sites. Several linear or branched electrophilic mPEG polymers of 12, 20, 30, and 40 kDa were included in the investigations of lysine modification, whereas, PEG-aldehyde was employed for N-terminal modification. Di- and tri-PEGylated IFN-β-1b proteins were also prepared for comparison to the preferred mono-PEGylated compounds.

Previous studies of PEGylation of IFN-α and IFN-β-1a demonstrate the utility in either random or site-specific modification with one large PEG polymer per protein (*40*, *41*, *43*, *46*). Since IFN-β-1b exhibits only about 35% sequence identity with the IFN-α family, and lacks the N-glycan, N-terminal methionine, and free thiol of IFN-β-1a, there may be limited guidance in the PEGylation approach for IFN-β-1b from these prior studies with other interferons.

Chart 1 displays the structures of the amine selective PEG polymers used in this study. These reagents react with primary amines with release of either the *N*-hydroxysuccinimide (NHS) or thiazolidine-2-thione (T) leaving group to form an acylated product. One example of bioconjugation of UA-PEG to primary amines is shown in Scheme 1. As shown in Figure 1A, eleven lysines and the N-terminal α-amine are available for modification by the well characterized activated PEG compounds such SC−PEG (*33*), XUS−PEG (*35*), T-PEG (*36*), and various NHS derivatives (*29*, *40*, *50*). ALD-PEG polymers may be employed to construct PEG conjugates selectively modified at low pH at the N-terminus, forming secondary amines by reduction with sodium cyanoborohydride (*37*, *46*). Mono-PEGylation of proteins using random amine-directed chemistries commonly produces positional isomers, which are conjugate mixtures with single PEG attachments at different sites on the protein surface. We conducted trypsin or Lys-C peptide mapping analysis, amino acid sequence analysis, LC/MS, and MALDI-TOF or SELDI-TOF MS on two of the most promising mono-PEGylated conjugates, which employed the branched 40 kDa PEG_2−NHS or 40 kDa PEG_2-ALD polymers, to evaluate preferred linkage sites. Figure 1B summarizes the major sites of attachment for these derivatives.

The 40 kDa ALD PEG_2 selectively modified the N-terminus; minor alternate sites (<15%) were not identified. Conjugation with the 40 kDa NHS PEG_2 polymer produced at least five major positional isomers corresponding to positions S1 plus K18 (42%), K104 (18%), K32 (15%), and K133 (14%), and other sites (11%). The N-terminal sequence analyses indicated that K18 was a slightly more preferred PEGylation site than the alpha amine of serine-1 on this N-terminal peptide. The structure of IFN-β-1a shows that the lysines with the most solvent exposed amino groups are K18, K107, and K133. Two of these lysines were shown in these analyses to be PEGylated in NHS 40 kDa PEG_2−IFN-β-1b. K107 is located within a tripeptide Lys-C fragment that eluted very early during C18 RP-HPLC, and this precluded a conclusive determination for this position. The available data suggest that K107, although well exposed, may be a minor site for PEGylation in this compound.

Using systematic mutational mapping of IFN-β-1a, Runkel et al. (*3*, *4*) proposed binding sites for the type I IFN (IFNAR-

Chart 1. Amine-Selective PEG Reagents

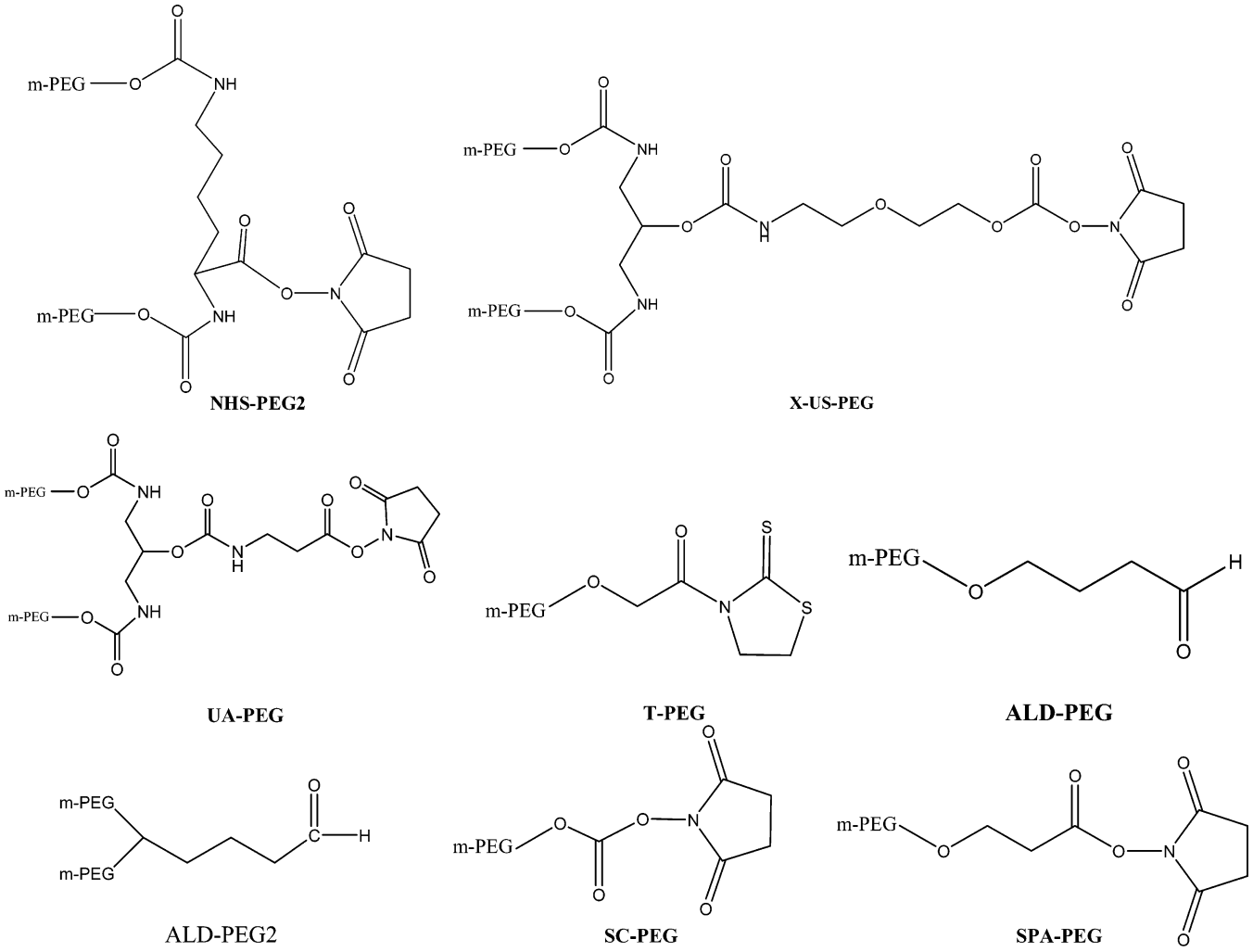

Scheme 1. Reaction of UA-PEG with Amine of Protein To Form an Amide Linkage

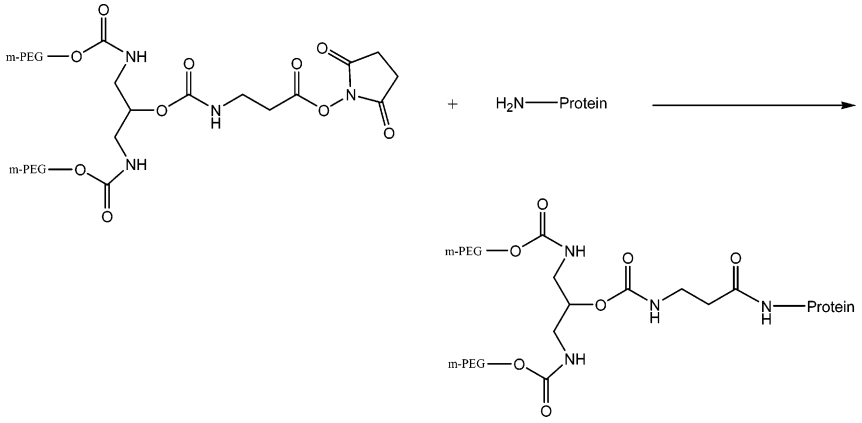

1/IFNAR-2) receptor from Daudi cells. For example, K18, K32, K122, and K133 are located in the general proximity of the binding site for IFNAR-2 and PEGylation at these sites might compromise the efficiency of receptor binding to PEG−IFN-β-1b. For the purpose of our present investigations, the observed differences in distribution of positional isomers in these two conjugates provide a basis for subsequent comparison of functional properties in relationship to structural differences.

We also examined two alternate, entirely site-specific PEGylation approaches for PEG−IFN-β-1b engineering that were both found to be unsatisfactory in our investigations. A recent trend in PEGylation has been the generation of site-specific modification with a single large polymer (*40*, *43*, *49*). Designed protein variants containing one free cysteine may be effectively conjugated to maleimide activated polymers (*28*). We designed three such variants of IFN-β-1b wherein the free cysteine is engineered at either the N-terminus, the C-terminus, or at position 79, which is occupied by the N-glycan in the native protein (Figure 1B). All proteins were expressed and purified in similar yields and bioactivities, compared to IFN-β-1b. However, a completely site-specific modification with maleimide PEG polymers, by our previous protocol (*28*), proved to be challenging due to the lability of the protein disulfide (C30−C140) under reducing conditions. Although conducting the

Table 1. Composition and Antiviral Activity of PEG−IFN-β-1b Conjugates

compound	IFN-β (%)[a]	mono PEG−IFN-β (%)[a]	di PEG−IFN-β (%)[a]	tri PEG−IFN-β (%)[a]	antiviral activity (%)[b]
native IFN-β−1b	100	0	0	0	100
mono NHS-40k-PEG_2−IFN	1	96	3	0	24
mono NHS-40k-PEG_2−IFN	1	97	2	0	22
mono NHS-40k-PEG_2−IFN	0.6	99	0	0.4	31
di NHS-40k-PEG_2−IFN	0	1	96	3	<1
mono ALD-20k-PEG−IFN	3	94	3	0	66
mono ALD-30k-PEG−IFN	0	99	1	0	58
mono ALD-40k-PEG_2−IFN	2	96	2	0	19
mono ALD-40k-PEG_2−IFN	0	99	0.6	0.4	25
mono T-12k-PEG−IFN	1	80	19	0	62
di T-12k-PEG−IFN	1	13	78	8	41
mono T-20k-PEG−IFN	1	96	3	0	55
di T-20k-PEG−IFN	0	8	84	8	23
mono UA-24k-PEG−IFN	1	94	3	2	43
mono UA-40k-PEG−IFN	0	96	3	1	35
mono XUS-40k-PEG−IFN	1	96	2	1	21
mono SC-12k-PEG−IFN	3	87	10	0	71
di SC-12k-PEG−IFN	1	12	82	5	26
tri SC-12k-PEG−IFN	0	0	4	96	1
mono SPA-20k-PEG−IFN	2	92	6	0	68
mono SPA-20k-PEG−IFN	1	94	5	0	63
di SPA-20k-PEG−IFN	0	4	91	5	21

[a] Following purification as described in Experimental Procedures of mono-, di-, and tri-PEG−IFN-β-1b derivatives, which contain one, two, or three PEG attachments per protein, respectively, the purified compounds were analyzed by SE-HPLC. The molar percent of each species in the purified compounds is based on SE-HPLC peak integration. In some cases, independent lots of a compound are shown. [b] The percent of antiviral activity per protein retained in the purified conjugates relative to native IFN-β-1b (30 MIU/mg = 100%).

conjugation reaction at acidic pH or with mild reducing reagents improved the maintenance of the disulfide linkage, the overall yield and complete site specificity of attachment were determined to be insufficient (data not shown).

Another reported approach for site-specific modification was described by Yamamoto et al. (*52*), wherein lysine depleted muteins were screened, thus producing variants with one or a few available primary amines. Our attempts to use this protocol with IFN-β-1b variants demonstrated limited success. Most variant proteins lost antiviral activity or maintained an unacceptably low residual activity such as the mutein shown in Figure 1B which retained only 1% of the native bioactivity. Therefore, we focused our detailed investigations of PEGylated IFN-β-1b on conventional amine selective chemistries under controlled reaction conditions.

PEGylation of IFN-β-1b. Amine directed PEGylation reactions and purification of either mono-PEGylated or di-PEGylated IFN-β-1b conjugates are described in Experimental Procedures. Seven previously described linker designs (*33*, *35*, *36*, *37*, *40*) were investigated including NHS, X-US, UA, T, SC, SPA and ALD. Four PEG masses were examined including 12 kDa, 20 kDa, 30 kDa, and 40 kDa. Table 1 summarizes the purity and bioactivity of the PEGylated IFN-β-1b derivatives investigated in a first screen of compounds. Isolation of mono-PEGylated derivatives was possible from the starting conjugate mixtures, with native IFN-β-1b and di- and tri-PEGylated conjugates present as either trace impurities or as significant species, depending on the conjugate category. The purification of the multi-PEGylated derivatives allowed an initial examination of the correlation of degree of modification with bioactivity. Figure 2 presents one representative SDS−PAGE analysis, including Coomassie Blue, Western, and iodine staining, of mono-PEGylated IFN-β-1b compounds with 12 kDa, 20 kDa, or 40 kDa polymers.

Relative to native IFN-β-1b, the mono-PEGylated compounds retained excellent activity. The retention of about 20−70% of antiviral activity in these derivatives compares favorably to the marketed PEGylated IFN-α drugs, PEG-INTRON and Pegasys, where in vitro antiviral activities are about 28% or 7% of the unmodified protein, respectively (*40*, *45*). It is apparent that the conjugates with the highest molecular weight 40 kDa PEG polymers have lower antiviral activity in vitro. There is no apparent distinction between different linkers and bioactivity within the mono-PEGylated derivatives. A significant observa-

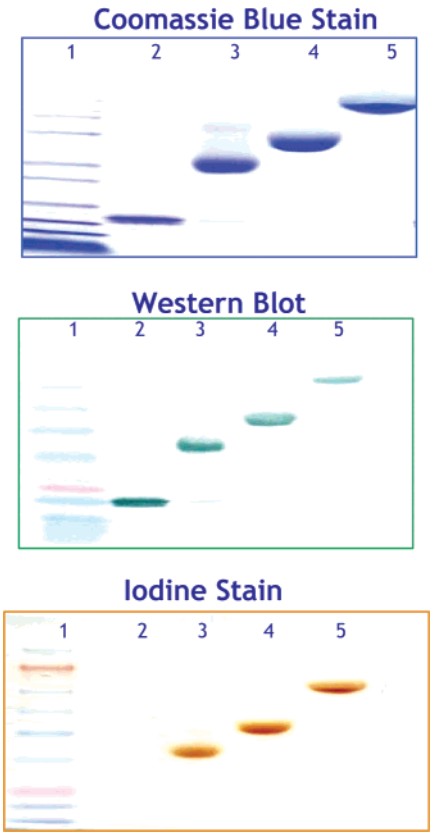

Figure 2. SDS−PAGE analysis of mono-PEGylated IFN-β-1b compounds. Molecular weight markers (lane 1), IFN-β-1b (lane 2), SC 12 kDa PEG−IFN-β-1b (lane 3), SPA 20 kDa PEG−IFN-β-1b (lane 4), and NHS 40 kDa PEG_2−IFN-β-1b (lane 5) are shown. The samples were denatured by heating at 85 °C for 3 min in the presence of 12 mM β-mercaptoethanol. Protein was identified by Coomassie Blue staining or Western staining with anti-huIFN-β mAb; PEG was detected by iodine staining.

Table 2. Molecular Mass of PEG−IFN-β-1b Compounds

compound	MALDI-TOF	SEC[a]	SEC PEG std[b]	SDS−PAGE	calculated[c]
native IFN-β−1b	19876	20000	n.a.	20000	19878
mono SC-12k-PEG−IFN-β	32000	401000	36000	39000	32000
di SC-12k-PEG−IFN-β	40000	430000	38000	54000	44000
mono T-20k-PEG−IFN-β	40000	401000	36000	51000	40000
mono SPA-20k-PEG−IFN-β	40000	430000	38000	50000	40000
di SPA-20k-PEG−IFN-β	60000	874000	65000	110000	60000
mono ALD-20k-PEG−IFN-β	40000	317000	31000	49000	40000
mono ALD-30k-PEG−IFN-β	50000	596000	49000	60000	50000
mono ALD-40k-PEG_2−IFN-β	60000	894000	66000	115000	60000
mono NHS-40k-PEG_2−IFN-β	60000	876000	65000	120000	60000

[a] Molecular weight determined with protein standard markers. [b] Molecular weight determined with PEG polymer standard markers. [c] Molecular weight determined from DNA sequence plus estimated polymer mass.

tion from this study is the reduced or abolished in vitro bioactivity for the multi-PEGylated IFN-β-1b compounds. Attachment of two 40 kDa branched polymers, or attachment of three 12 kDa linear polymers diminished antiviral activities by about 100-fold. Independent analysis of bioactivity of the compounds by an anti-proliferation assay on A549 cells provided similar results (data not shown).

One especially interesting conjugate is the SPA 2 × 20 kDa di PEGylated IFN-β-1b compound, which does retain 21% of native antiviral activity. This conjugate is analogous to the branched 40 kDa PEG modified protein, except the two 20 kDa polymers are at disparate sites rather than at a common attachment position. Therefore, comparison of biological properties of these two conjugate types will be instructional. In addition to the isolation of conjugate species, the purification protocol was also able to remove free PEG polymers, SDS, and Zwittergent, as verified by light scattering detection, acridine orange assays, and RP-HPLC, respectively. Additional purity analysis of these conjugates, including analysis of endotoxin (<1 EU/mL) and *E. coli* protein contaminants (<15 ppm), were conducted prior to in vivo studies.

As shown in Table 2, MALDI-TOF MS confirmed the predicted molecular mass of IFN-β-1b and PEG−IFN-β-1b compounds, and gel filtration analysis demonstrated the capacity of PEGylated proteins to markedly expand in hydrodynamic volume resulting in a predicted molecular weight about 14-fold greater than the calculated mass in the case of the conjugates with single 40 kDa branched polymer attachments. Use of PEG polymer or PEG-protein standards also allowed an approximate measurement of mass with SEC or SDS−PAGE methods, respectively. An evaluation of the preliminary compounds in Table 1 and Table 2 was the basis for selection of several of these conjugates for further analytical and pharmacological investigations.

Stability, Solubility, and Aggregation Analysis. Marketed interferon-β drugs have encountered formulation challenges for this aggregation prone protein; Betaseron, Avonex, and Rebif are formulated with human serum albumin either as powder or in solution. One of the potential benefits of PEGylation for an exceptionally hydrophobic protein such as IFN-β-1b, which is particularly susceptible to aggregation, is increasing the solubility and stability of the conjugate molecule. This attribute was immediately apparent in our investigations of PEGylated IFN-β-1b conjugates. When native IFN-β-1b was formulated in aqueous solution in the absence of a surfactant, such as Zwittergent 3−14, the protein rapidly and quantitatively precipitated as insoluble aggregates within 7 days at neutral pH, whereas the 40 kDa PEGylated IFN-β-1b remained soluble during this duration. Using the selected formulation buffer (3 mM HAc, pH 3.7, 5% mannitol), we found that the NHS 40 kDa PEG_2−IFN-β-1b compound retained the initial antiviral bioactivity (8.5 MIU/mg ± 20%) for 6 months when stored in aqueous solution at 4 °C.

However, we wished to perform a stringent analysis of the physical behavior of PEG−IFN-β in stability studies in order to also examine the extent of formation of soluble aggregates of the bioconjugate. We used RP-HPLC to examine the physical integrity and purity of the conjugates, and SE-HPLC to examine the appearance of soluble aggregates in the PEG−IFN-β-1b preparations. As shown in Figure 3A and 3B, the chromatographic analyses distinguished the mono-PEGylated protein from both degradation products and aggregates. As shown in Table 3, the NHS 40 kDa PEG_2−IFN-1b compound (0.1 mg protein/ml) demonstrated no formation of soluble aggregates during 37-day storage at 4 °C at pH 3.7−4.0. However, storage at higher pH (5.0−8.5) resulted in increasing formation of soluble aggregates with higher pH. We further examined the stability of PEGylated IFN-β-1b compounds in plasma and confirmed no significant loss of antiviral activity in rat plasma incubated at 37 °C for 72 h for the seven conjugates used in subsequent in vivo studies. There was a trend toward better in vitro solubility and stability of the IFN-β-1b conjugates with increasingly higher molecular weight polymers. This may be compared to the successful formulation of the relatively more soluble IFN-α proteins with PEG polymers of intermediate size. Additionally, we examined the rate of degradation of IFN-β-1b and PEG-modified counterparts in rat liver and kidney extracts at 37 °C. The rates of degradation of the PEGylated proteins were approximately 15% of the native protein based on antiviral activity measurements (data not shown).

Finally, we wanted to examine the conformational and structural integrity of the PEGylated IFN-β-1b in a direct comparison to the native protein. In circular dichroism analysis of the NHS 40 kDa PEG_2−IFN-β-1b compound and native IFN-β-1b (0.1 mg/mL), the CD spectra were indistinguishable. As shown in Figure 3C, in additional studies of thermal unfolding of the helices (α helix content ∼ 60%), the thermal stability of the protein and conjugate were very similar and the thermal unfolding of the helices was uncooperative in character. The melting temperatures of IFN-β-1b (T_m = 61.8 °C) and two independent preparations of 40 kDa PEG_2−IFN-β-1b (T_m = 63.2 °C; T_m = 63.5 °C) were virtually identical. The CD data confirm that PEGylation does not impart a notable alteration in secondary structure or thermal stability of the IFN-β-1b protein.

Pharmacokinetic Analysis in Mice and Rats. A hallmark of the beneficial effects of PEGylation is an increased blood residency time of the bioconjugates. Pharmacokinetic properties of the IFN-β-1b and PEGylated IFN-β-1b compounds were determined in both mice and rats using antiviral bioassays for quantitation. While immunoassay methods for detection of total compound produced comparable results for the PEGylated derivatives, native IFN-β-1b cleared too rapidly for detection by ELISA. Three routes of administration—intravenous, subcutaneous, and intramuscular—were examined in both rats and mice. A comparison of the PK profiles in mice of native IFN-β-1b and the amine directed mono-PEGylated conjugates with

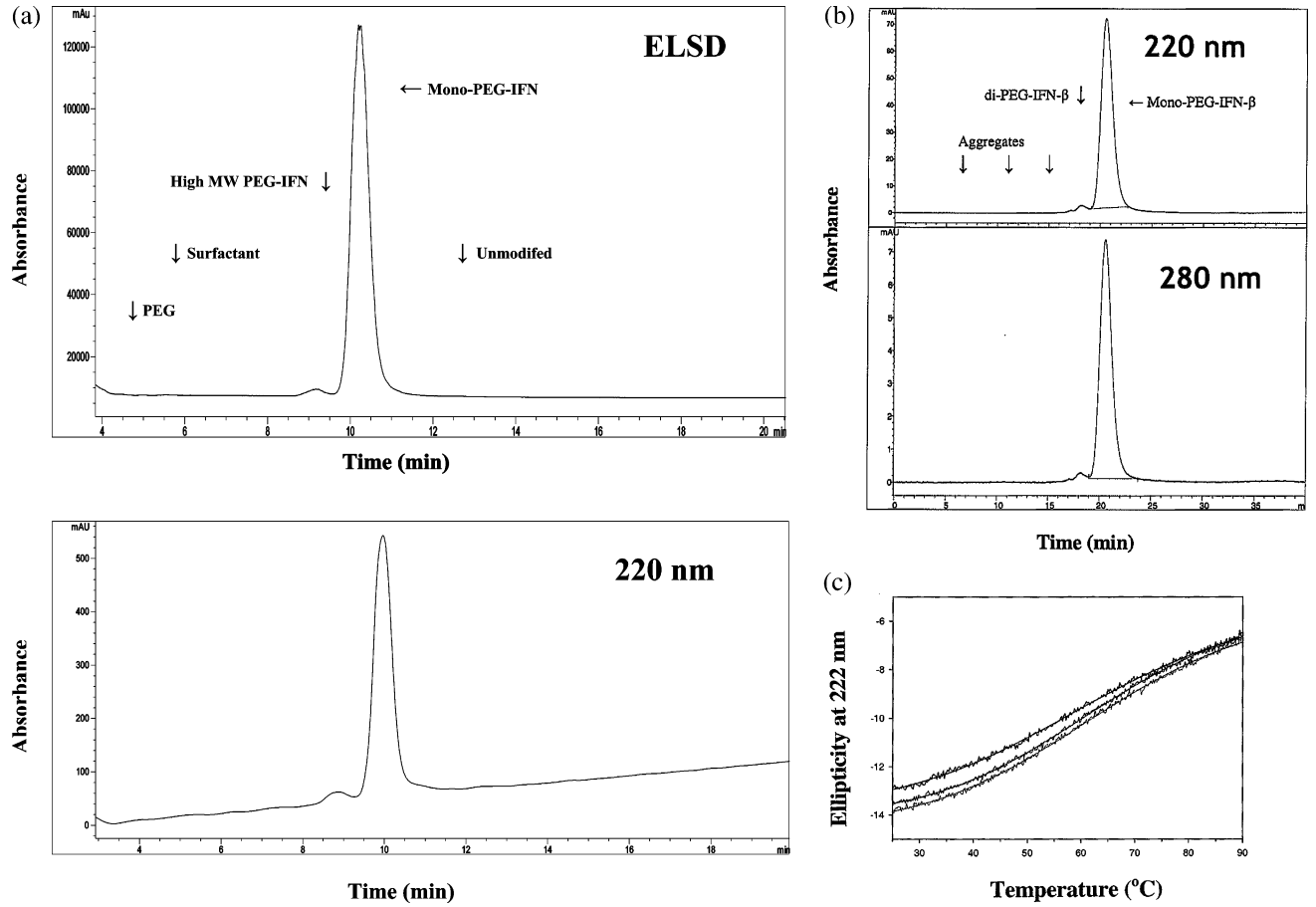

Figure 3. Analyses of physical integrity of PEG−IFN-β-1b. (A) RP-HPLC of NHS 40 kDa PEG_2−IFN-β-1b (0.48 mg/mL in 5% mannitol, 3 mM HAc, pH 3.7) on Vydac C4 at 55 °C with diode array and evaporative light scattering detectors. Upper graph is ELSD scan; lower graph is generated by a 220 nm UV detector. Buffer A: 0.1% TFA in H_2O; buffer B: 0.1% TFA in acetonitrile; gradient: 45−60% over 25 min; flow rate: 0.80 mL/min. Elution times of each species are shown. (B) SE-HPLC of NHS 40 kDa PEG_2−IFN-β-1b (0.88 mg protein/mL in 5% mannitol, 3 mM HAc, pH 3.7) on Superdex 200 HR at 24 °C. Running buffer is 100 mM sodium phosphate, pH 6.8; flow rate is 0.50 mL/min. Elution times of each species are shown. UV detectors scanned 220 nm (upper) and 280 nm (lower). (C) Circular dichroism analysis of IFN-β-1b (upper curve) and two independent preparations of NHS 40 kDa PEG_2−IFN-β-1b (lower two curves) in thermal denaturation investigations. Samples were 0.1 mg/mL (protein) in 5 mM HAc buffer, pH 3.7; CD was conducted at 25 °C. Ellipticity at 222 nm as a function of temperature (°C) is shown.

Table 3. Effect of Buffer pH of 40 kDa PEG_2−IFN-β-1b on Aggregation[a]

buffer	concentration, mM	pH	protein (mg/mL)	T (°C)	time (day)	aggregation (%)
acetic acid	3	3.7	0.1	4	37	0.0
citrate	5	4.0	0.1	4	37	0.0
citrate	5	5.0	0.1	4	37	3.5
citrate	5	6.0	0.1	4	37	4.1
phosphate	5	7.4	0.1	4	37	6.7
phosphate	5	8.5	0.1	4	37	57.3
H_2O		6.5	0.1	4	37	4.7

[a] Percent aggregates of mono-PEGylated NHS-40k-PEG_2−IFN were measured by SE-HPLC.

either NHS 40 kDa PEG_2, SPA 20 kDa PEG, or SC 12 kDa PEG polymers is shown in Figure 4A. Total exposure of the protein is markedly enhanced through PEGylation, and the rank order of exposure increased with increasing PEG mass. In Figure 4B, a similar trend is observed with the mono-PEGylated compounds employing aldehyde linkers. Greatest exposure is observed with the branched 40 kDa ALD-PEG polymer, while the native IFN-β-1b exposure is marginal. In all sets of PK experiments, a second control using Betaseron was included to confirm the comparability of the PK profile of the experimental IFN-β-1b protein (data not shown). As shown in Figure 4C, the mouse PK profile exhibited a similar outcome in side-by-side comparison of the 40 kDa PEG conjugates, including mono-PEGylated derivatives of NHS−PEG_2, ALD-PEG_2, UA-PEG, XUS−PEG, and a di-PEGylated derivative of SPA-20 kDa polymers. Native IFN-β-1b cleared rapidly from the mice, whereas each of the high molecular weight conjugates exhibited very similar absorption and elimination curves. Mice were administered 0.2 mg protein/kg of all compounds, or about 4 μg of interferon protein per mouse. Since the PEGylated IFN-β-1b compounds do not contain equivalent antiviral activity compared the native interferon, as shown in Table 1, the PEGylated conjugates were actually under-dosed relative the native control, with respect to units of activity. In some cases, subsequent conversions of units of bioactivity to ng of protein were performed with an internal standard for specific activity for each individual compound, corresponding to the analyzed sample administered to the animal. Table 4 presents representative pharmacokinetic parameters from the subcutaneous administration route in mice. All PEGylated conjugates exhibit an expanded area under the curve, relative to unmodified protein, of about 14-fold to 173-fold, which increases with polymer mass. The times of maximal concentration by the sc route were delayed in all of the PEGylated compounds by several hours relative to native IFN-β-1b.

The PEG_2-40 kDa polymers demonstrated exceptionally good performance and were selected for detailed studies in PK studies in rats. Figure 5A shows the side-by-side comparison of PK profiles of PEGylated IFN-β-1b compounds with 40 kDa mass

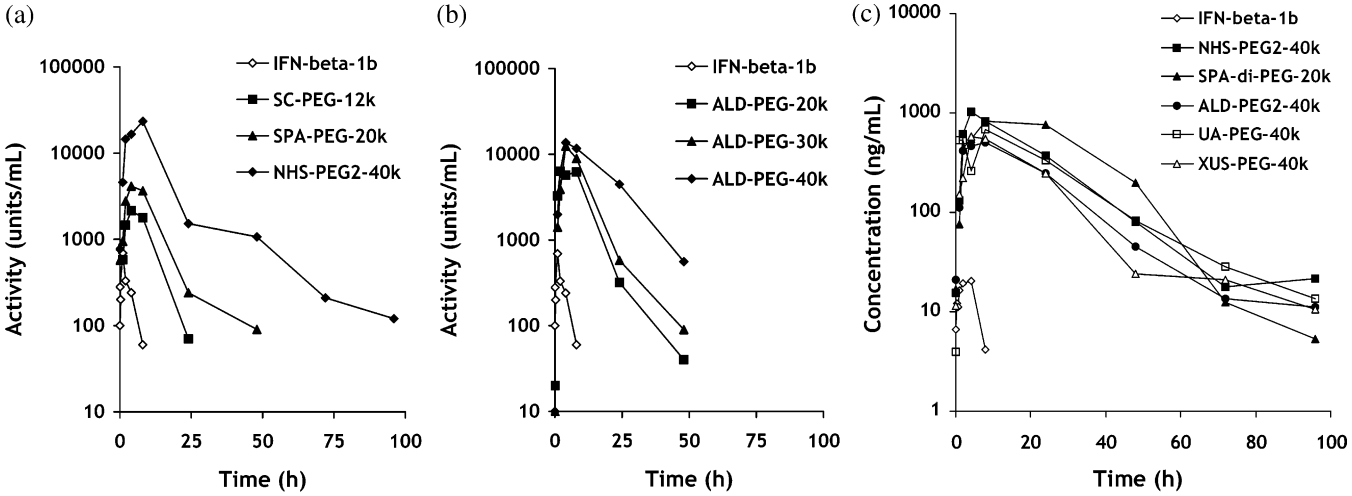

Figure 4. Pharmacokinetics of IFN-β-1b and mono-PEGylated IFN-β-1b in mice. (A) Subcutaneous administration at 0.2 mg protein/kg for IFN-β-1b (open diamonds), NHS 40 kDa PEG_2−IFN-β-1b (closed diamonds), SPA 20 kDa PEG−IFN-β-1b (closed triangles), SC 12 kDa PEG−IFN-β-1b (closed boxes). Antiviral activity of plasma samples was measured at the indicated times post-administration. (B) PK profile of IFN-β-1b (open diamonds), ALD 40 kDa PEG_2−IFN-β-1b (closed diamonds), ALD 30 kDa PEG−IFN-β-1b (closed triangles), ALD 20 kDa PEG−IFN-β-1b (closed boxes) at 0.2 mg/kg dose following sc administration. (C) PK profile of IFN-β-1b (open diamonds), NHS 40 kDa PEG_2−IFN-β-1b (closed boxes), ALD 40 kDa PEG_2−IFN-β-1b (closed circles), X-US 40 kDa PEG−IFN-β-1b (open triangles), UA 40 kDa PEG−IFN-β-1b (open boxes) and di-PEGylated SPA 2 × 20 kDa PEG−IFN-β-1b (closed triangles) at 0.2 mg/kg dose following sc administration.

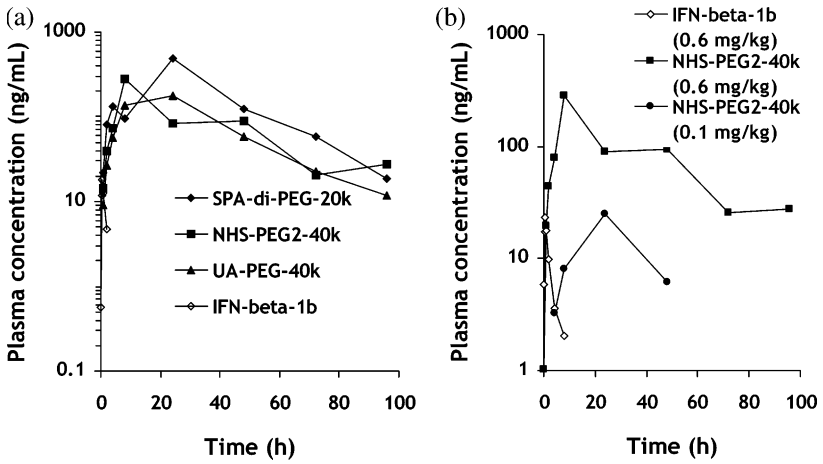

Figure 5. Pharmacokinetics of IFN-β-1b and mono-PEGylated IFN-β-1b in rats. (A) Subcutaneous administration at 0.6 mg protein/kg for IFN-β-1b (open diamonds), NHS 40 kDa PEG_2−IFN-β-1b (closed boxes), UA 40 kDa PEG−IFN-β-1b (closed triangles), and di-PEGylated SPA 2 × 20 kDa PEG−IFN-β-1b (closed diamonds). Antiviral activity of plasma samples was measured at the indicated times post-administration. (B) Dose−response for NHS 40 kDa PEG_2−IFN-β-1b at 0.6 mg protein/kg (closed boxes) or 0.1 mg protein/kg (closed circles) following sc administration. Unmodified IFN-β-1b (0.6 mg/kg) is also shown (open diamonds).

Table 4. Pharmacokinetic Parameters in Mice[a]

compound	route	dose (mg/kg)	AUC (h·U/mL)	T_{max} (h)
IFN-β−1b	sc	0.2	2040	0.9
NHS-40k-PEG_2−IFN	sc	0.2	352740	6.3
SC-12k-PEG−IFN	sc	0.2	27920	5.1
SPA-12k-PEG−IFN	sc	0.2	58180	3.7
ALD-20k-PEG−IFN	sc	0.2	88680	4.4
ALD-30k-PEG−IFN	sc	0.2	157100	5.9
ALD-40k-PEG_2−IFN	sc	0.2	258440	7.3
di SPA-20k-PEG−IFN	sc	0.2	103854	13.0

[a] PK parameters of mono-PEGylated IFN-β-1b compounds and di-PEGylated SPA (2 × 20 kDa) PEG−IFN-β-1b compound were determined by using a two-compartment, first-order input, first-order elimination model. AUC, area under the curve; T_{max}, time of maximal concentration postadministration.

of PEG polymers per protein, but with three different linker chemistries and conformations. The two mono-PEGylated compounds, PEG_2-40 kDa and PEG-UA-40 kDa, employ an NHS ester on a branched polymer and generate an amide linkage, while the di-PEGylated IFN-β-1b compound uses a 20 kDa PEG with an SPA linker, and two random amide linkages with 20 kDa PEG polymers are formed in this PEG−IFN-β-1b compound. The PK results are comparable for these three compounds, which all demonstrated much greater exposure than the unmodified interferon. A dose−response investigation in rats, shown in Figure 5B, demonstrated that the AUC exposure of 40 kDa PEG_2−IFN-β-1b was relative to the administered dose. Rats receiving 0.1 mg/kg or 0.6 mg/kg of this compound displayed an AUC difference of 9-fold. Table 5 summarizes key PK parameters for two representative mono-PEGylated 40 kDa PEG−IFN-β-1b compounds administered to rats via the three routes of injection. Both molecules demonstrated comparable overall performance as sc or im administered compounds. Both bioconjugates displayed comparable terminal half-lives (18−23 h in sc route), while exhibiting an expanded Tmax (24−48-fold increase via sc) and increased Cmax (9−19-fold increase via sc) relative to the native protein. Similarly, the clearance via the sc route for the two PEGylated conjugates was diminished 125−210-fold relative the unmodified interferon. PK parameters for the di-PEGylated SPA-20 kDa-PEG−

Table 5. Pharmacokinetic Parameters in Rats[a]

compound	route	dose (mg/kg)	half-life (h)	AUC (h.U/mL)	CL (mL/h) × (μg/U)	T (h)	C_{max} (U/mL)
IFN-β−1b	iv	0.6	1.1	26210	0.0057	nd	nd
NHS-40k-PEG_2−IFN	iv	0.6	9.4	751328	0.0002	nd	nd
UA-40k-PEG−IFN	iv	0.6	12.0	687389	0.0002	nd	nd
IFN-β−1b	sc	0.6	2.4	324	0.3990	1.0	95
NHS-40k-PEG_2−IFN	sc	0.6	23.8	72014	0.0019	24	1829
UA-40k-PEG−IFN	sc	0.6	18.1	42938	0.0032	48	798
IFN-β−1b	im	0.6	2.3	805	0.1500	0.5	136
NHS-40k-PEG_2−IFN	im	0.6	15.2	164920	0.0009	8.0	4909
UA-40k-PEG−IFN	im	0.6	14.4	76782	0.0019	8.0	2990

[a] PK parameters of the mono-PEGylated IFN-β-1b compounds: AUC, area under the curve; CL, total body clearance; T_{max}, time of maximal concentration; C_{max}, maximal concentration; nd, not determined.

Table 6. Bioavailability of IFN-β-1b and PEG−IFN-β-1b Conjugate in Mice and Rats

		dose (mg/kg)		bioavailability (%)	
compound	species	sc	im, iv	sc	im
IFN-β−1b	mouse	0.2	0.1	15	30
NHS-40k-PEG_2−IFN-β-1b	mouse	0.2	0.1	22	42
IFN-β−1b	rat	0.6	0.6	1	3
NHS-40k-PEG_2−IFN-β-1b	rat	0.6	0.6	10	22

IFN-β-1b compound were similar to the conjugates with a single branched 40 kDa polymer (data not shown). The specific choice of preferred linker for the branched (2 × 20) kDa design might ultimately be based on practical considerations, such as ease and costs of synthesis.

One highlighted comparison of the three routes of administration with regard to bioavailability, based on total AUC exposure of activity units, is shown in Table 6. Bioavailability was superior for the 40 kDa PEG_2−IFN-β-1b conjugate compared to IFN-β-1b. The difference was greatest in rats where the bioconjugate exhibited 8-fold and 7-fold better bioavailability by sc and im routes, respectively. The overall bioavailability by im injection was excellent, which suggests this parenteral route might be an alternative to the currently used sc administration of Betaseron in patients. The enhanced exposure of the PEGylated IFN-β-1b compounds is expected to provide a much more potent drug than unmodified IFN-β-1b, with respect to AUC effects per mg of protein.

Immunogenicity in Rats. Immunogenicity is a central concern in the development and drug monitoring of protein therapeutics, including PEGylated proteins. Binding antibodies are commonly encountered, and neutralizing antibodies versus Betaseron and other IFN-β compounds have been reported (*17*−*22*). Measurement of the antibody response to a protein therapeutic is challenging. First, immunogenicity in animals is not sufficiently predictive of immunogenicity in humans. Second, an antidrug immune response may dissipate over time. Third, it is difficult to develop the perfect analytical method to measure an antibody response, since immunoassays normally measure titers, and the detection sensitivity of immunoassays will vary based in part on the affinity of the serum antibodies and test reagents. With these limitations in mind, we examined the immune response to IFN-β-1b and four PEGylated (40 kDa PEG) IFN-β-1b compounds in rats.

Rats received 0.1 mg/kg once weekly im injections of the compounds for six weeks. Rat plasma samples were collected each week and analyzed by direct ELISA, indirect ELISA, flow cytometry, Biacore, or antiviral activity neutralization. As shown in Figure 6A, the rat IgG response to the four PEGylated IFN-β-1b compounds was markedly diminished in week two through week six compared to the IgG response to unmodified IFN-β-1b. In this immunoassay, native IFN-β-1b coated the plates and the bound rat IgG was specifically detected by anti rat IgG reagents. Measurement of the antigen specific IgG antibody levels by direct ELISA was based on a control mAb versus human IFN-β. Direct ELISA analysis however demonstrated a similarity in IgM response for all compounds (data not shown). The rat plasma samples were also examined in an alternate capture ELISA format as shown in Figure 6B. Either IFN-β-1b or PEG−IFN-β-1b was captured on an anti human IFN-β mAb immobilized on the plate, and the plasma samples were analyzed on the plates for IFN-β-1b or PEG−IFN-β-1b binding IgG antibodies. High titers of IgG versus IFN-β-1b were produced in rats injected with the unmodified protein at week six, whereas much lower titers of IgG versus 40 kDa PEG_2−IFN-β-1b were produced in rats injected with the PEG conjugate. Most interestingly, the rat IgG antibodies versus native IFN-β-1b did not demonstrate significant binding to PEG−IFN-β-1b, whereas rat IgG versus PEG−IFN-β-1b did demonstrate significant binding to native IFN-β-1b. Since these ELISA plates were coated with an anti human IFN-β mAb, however, any rat plasma IgG directed against a common epitope to the immobilized anti−IFN-β mAb would likely be undetected in this immunoassay.

To further evaluate low affinity IFN-β-1b binding IgG, we performed analysis of the rat plasma samples by flow cytometry using cell line A549, which was incubated first with IFN-β-1b, and then with rat plasma and phycoerythrin conjugated anti-rat IgG reagents. As shown in Figure 6C, fluorescence measurements demonstrated that total IgG bound was greater in the plasma from rats injected with native IFN-β-1b. In Biacore analysis, IFN-β-1b was immobilized on the chip surface. Measurement of total bound antibodies, including IgM and low affinity IgG, also exhibited a trend to reduced titers in the plasma from rats injected with the PEGylated IFN-β-1b conjugate when compared to plasma from rats administered the unmodified protein (data not shown). Antiviral bioassays were employed to examine the capacity of the rat plasma samples to neutralize IFN-β-1b activity in cell culture. Neutralizing antibodies were detected at six weeks in plasma from rats injected with either the native or PEGylated protein, although the plasma from native IFN-β-1b produced a higher titer antibody response (data not shown). Also, rat antibodies raised versus either native or PEGylated IFN-β-1b were capable of neutralizing either the native or PEGylated interferon compounds.

Possibly, the immunoassay designs in Figures 6A and 6B detect a high affinity IgG response in the treated rats, whereas the remaining assays reflect the total high/low affinity IgG and IgM response. One concern for mono-PEGylated proteins is the potential for enhancement of the host immune response due to the large prolongation in blood residency time of the protein (*46*). This effect was not demonstrated in any of our studies. Rather, it seems possible that the solubilized and shielded PEGylated IFN-β-1b may be an inferior antigen for dendritic cells in sc or im administration compared to the aggregation-prone native protein. Further studies in primates and humans are needed to address the question of immunogenicity of these experimental compounds.

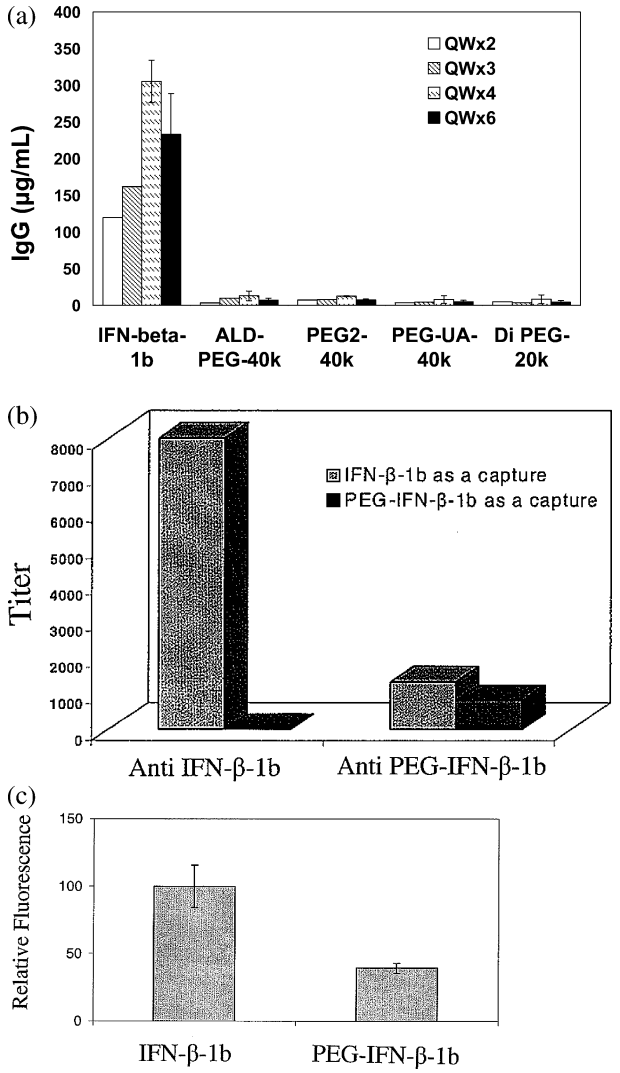

Figure 6. Immunogenicity of IFN-β-1b and PEGylated IFN-β-1b in rats. (A) IgG response, following weekly im injections (0.1 mg/kg), at weeks 2, 3, 4, and 6 to IFN-β-1b and four PEG−IFN-β-1b conjugates. QW × 2, QW × 3, QW × 4, and QW × 6 correspond to once per week dosing at weeks 2, 3, 4, and 6, respectively. IgG (μg/mL) were estimated based on a standard curve with anti-huIFN-β mAb MMHB-3. IFN-β-1b and PEG−IFN-β-1b compounds were coated on ELISA plates prior to incubation with rat plasma and anti-rat IgG-HRP conjugate. (B) Indirect (capture) ELISA assay of IgG response in rats to IFN-β-1b and NHS 40 kDa PEG_2−IFN-β-1b at week 6. Anti-huIFN-β mAb was immobilized on the plate to capture either native or PEGylated protein. Plasma from the rats injected with either of these two test articles were incubated independently on microtiter wells with the captured native or PEG IFN-β-1b, followed by detection with anti-rat IgG-HRP reagent. (C) Flow cytometry with relative fluorescence intensity results for A549 cells incubated with native IFN-β-1b, then incubated with rat plasma versus either native IFN-β-1b or NHS 40 kDa PEG_2−IFN-β-1b, and phycoerythrin-conjugated anti-rat IgG mAb.

CONCLUSIONS

We describe investigations of the physical and functional properties of mono-PEGylated IFN-β-1b compounds. Employment of PEGylation strategies for drug delivery often focus on one specific desired improvement in the drug features, and this is most often a need for improved circulating life. Our present studies illustrate the capacity of attachment of a PEG polymer to IFN-β-1b to improve five key attributes in the bioconjugate. In comparison to the unmodified protein, PEG−IFN-β-1b compounds exhibit better solubility, less propensity to insoluble and soluble aggregation, expanded in vivo exposure of bioactive protein, prolonged blood residency, and a reduced IgG response versus the bioconjugate. Many other protein ligands that have been proposed as therapeutics encounter similar challenges and these PEGylation strategies may be applicable in addressing formulation, stability, and pharmacology difficulties in other incommodious hydrophobic proteins. Our studies also illustrate both the difficulties in site-specific modification of engineered proteins and the ability to construct markedly differing bioconjugates, such as with either the 40 kDa mono-PEGylated NHS−PEG_2 and ALD-PEG_2 derivatives or the di-PEGylated SPA-(2 × 20 kDa) derivative, that nonetheless exhibited notably similar physical and biological properties. The mono-PEGylated IFN-β-1b compounds with a branched 40 kDa polymer appear especially beneficial with regard to prolonged blood circulation and in vitro stability. Of several promising bioconjugates in this study, we chose to further investigate the 40 kDa PEG_2−IFN-β-1b compounds in ongoing pharmacokinetic and pharmacodynamic studies in primates.

ACKNOWLEDGMENT

We thank Steve Youngster, Qing Dong, Lisa Hwang, Eun Jang, and Julia Zhu for performance of MALDI-TOF and LC-MS. We are also grateful to Anju Dang and Massy Rajabzadeh of Ciphergen, Inc. for assistance with SELDI-TOF-MS analysis. We thank Uli Grau and Pascal Bailon for their encouragement and support and Jack Lipman and Ivan Horak for a critical review of the manuscript.

LITERATURE CITED

(1) Theofilopoulos, A. N., Baccala, R., Beutler, B., and Kono, D. H. (2005) Type I interferons (α/β) in immunity and autoimmunity. *Annu. Rev. Immunol. 23*, 307−336.

(2) Meager, A. (1998) Interferons alpha, beta, and omega. In *Cytokines* (Mire-Sluis, A. R., and Thorpe, R., Eds.) pp 361−389, Academic Press, San Diego.

(3) Runkel, L., deDios, C., Karpusas, M., Betzenhauser, M., Muldowney, C., Zafari, M., Benjamin, C. D., Miller, S., Hochman, P. S., and Whitty, A. (2000) Systematic mutational mapping of sites on human interferon-β-1a that are important for receptor binding and functional activity. *Biochemistry 39*, 2538−2551.

(4) Runkel, L., deDios, C., Karpusas, M., Baker, D., Li, Z., Zafari, M., Betzenhauser, M., Muldowney, C., Miller, S., Redlich, P. N., Grossberg, S. E., Whitty, A., and Hochman, P. S. (2001) Mapping of IFN-beta epitopes important for receptor binding and biologic activation: comparison of results achieved using antibody-based methods and alanine substitution mutagenesis. *J. Interferon Cytokine Res. 21*, 931−941.

(5) Arduini, R. M., Strauch, K. L., Runkel, L. A., Carlson, M. M., Hronowski, X., Foley, S. F., Young, C. N., Cheng, W., Hochman, P. S., and Baker, D. P. (1999) Characterization of a soluble ternary complex formed between human interferon-beta-1a and its receptor chains. *Protein Sci. 8*, 1867−1877.

(6) Mager, D. E., Neuteboom, B., Efthymiopoulos, C., Munafo, A., and Jusko, W. J. (2003) Receptor-mediated pharmacokinetics and pharmacodynamics of interferon-β1a in monkeys. *J. Pharmacol. Exp. Ther. 306*, 262−270.

(7) Durelli, L., Verdun, E., Barbero, P., Bergui, M., Versino, E., Ghezzi, A., Montanari, E., Zaffaroni, M., and the Independent Comparison of Interferon (INCOMIN) Trial Study Group. (2002) Every-other-day interferon beta-1b versus once-weekly interferon beta-1a for multiple sclerosis: results of a 2-year prospective randomized multicentre study (INCOMIN). *Lancet 359*, 1453−1460.

(8) Bertolotto, A., Deisenhammer, F., Gallo, P., and Sørensen, P. S. (2004) Immunogenicity of interferon beta: differences among products. *J. Neurol. 251*, II/15-II/24.

(9) Runkel, L., Meier, W., Pepinsky, R. B., Karpusas, M., Whitty, A., Kimball, K., Brickelmaier, M., Muldowney, C., Jones, W., and Goelz, S. E. (1998) Structural and functional differences between

glycosylated and nonglycosylated forms of human interferon-beta (IFN-beta). *Pharm. Res*. *15*, 641−649.
(10) Antonetti, F., Finocchiaro, O., Mascia, M., Terlizzese, M. G. and Jaber, A. (2002) A comparison of the biologic activity of two recombinant IFN-beta preparations used in the treatment of relapsing-remitting multiple sclerosis. *J. Interferon Cytokine Res*. *22*, 1181−1184.
(11) Horowski, R. (2002) Multiple sclerosis and interferon beta-1b, past, present and future. *Clin. Neurol. Neurosurg. 104*, 259−264.
(12) Williams, G. J. and Witt, P. L. (1998) Comparative study of the pharmacodynamic and pharmacologic effects of Betaseron and AVONEX. *J. Interferon Cytokine Res. 18*, 967−975.
(13) Mark, D. F., Lu, S. D., Creasey, A. A., Yamamoto, R. and Lin, L. S. (1984) Site-specific mutagenesis of the human fibroblast interferon gene. *Proc. Natl. Acad. Sci. U.S.A. 81*, 5662−5666.
(14) Chiang, J., Gloff, C. A., Yoshizawa, C. N. and Williams, G. J. (1993) Pharmacokinetics of recombinant human interferon-beta ser in healthy volunteers and its effect on serum neopterin. *Pharm. Res. 10*, 567−572.
(15) Karpusas, M., Nolte, M., Benton, C. B., Meier, W., Lipscomb, W. N., and Goelz, S. (1997) The crystal structure of human interferon β at 2.2-Å resolution. *Proc. Natl. Acad. Sci. U.S.A. 94*, 11813−11818.
(16) Karpusas, M., Whitty, A., Runkel, L., and Hochman P. (1998) The structure of human interferon-β: implications for activity. *CMLS. Cell. Mol. Life Sci. 54*, 1203−1216.
(17) Bertolotto, A., Gilli, F., Sala, A., Capobianco, M., Malucchi, S., Milano, E., Melis, F., Marnetto, F., Lindberg, R. L. P., Bottero, R., Di Sapio, A., and Giordana, M. T. (2003) Persistent neutralizing antibodies abolish the interferon β bioavailability in MS patients. *Neurology 60*, 634−639.
(18) Sorensen P. S., Ross C., Clemmesen, K. M., Bendtzen, K., Frederiksen, J. L., Jensen, K., Kristensen, O., Petersen, T., Rasmussen, S., Ravnborg, M., Stenager, E., Koch-Henriksen, N., and the Danish Multiple Sclerosis Study Group. (2003) Clinical importance of neutralizing antibodies against interferon beta in patients with relapsing-remitting multiple sclerosis. *Lancet 362*, 1184−1191.
(19) Bitsch, A., Dressel, A., Meier, K., Bogumil, T., Deisenhammer, F., Tumani, H., Kitze, B., Poser, S., and Weber, F. (2004) Autoantibody synthesis in primary progressive multiple sclerosis patients treated with interferon beta-1b. *J. Neurol. 251*, 1498−1501.
(20) Hartung, H.-P., Schellekens, H., and Munschauer III, F. E. (2004) Neutralizing antibodies to interferon beta in patients with multiple sclerosis: scientific background and clinical implications. *J. Neurol. 251*, II/1−II-3.
(21) Reske, D., Walser, A., Haupt, W. F., and Petereit, H.-F. (2004) Long-term persisting interferon beta-1b neutralizing antibodies after discontinuation of treatment. *Acta Neurol. Scand. 109*, 66−70.
(22) Yeung, V. P., Chang, J., Miller, J., Barnett, C., Stickler, M. and Harding, F. A. (2004) Elimination of an immunodominant $CD4^+$ T cell epitope in human IFN-β does not result in an in vivo response directed at the subdominant epitope. *J. Immunol. 172*, 6658−6665.
(23) Runkel, L., Pfeffer, L., Lewerenz, M., Monneron, D., Yang, C. H., Murti, A., Pellegrini, S., Goelz, S., Uzé, G., and Mogensen, K. (1998) Differences in activity between α and β type I interferons explored by mutational analysis. *J. Biol. Chem. 273*, 8003−8008.
(24) Goldman, L. A., Zafari, M., Cutrone, E. C., Dang, A., Brickelmeier, M., Runkel, L., Benjamin, C. D., Ling, L. E. and Langer, J. A. (1999) Characterization of antihuman IFNAR-1 monoclonal antibodies: epitope localization and functional analysis. *J. Interferon Cytokine Res*. *19*, 15−26.
(25) David, M. (2002) Signal transduction by Type I interferons. *BioTechniques 33*, S58−S65.
(26) Khan, O. A., Xia, Q., Bever, C. T. Jr., Johnson, K. P., Panitch, H. S., and Dhib-Jalbut, S. S. (1996) Interferon beta-1b serum levels in multiple sclerosis patients following subcutaneous administration. *Neurology*, *46*, 1639−1643.
(27) Greenwald, R. B. (2001) PEG drugs: an overview. *J. Controlled Release 74*, 159−171.
(28) Yang, K., Basu, A., Wang, M., Chintala, R., Hsieh, M.-C., Liu, S., Hua, J., Zhang, Z., Zhou, J., Li, M., Phyu, H., Petti, G., Mendez, M., Janjua, H., Peng, P., Longley, C., Borowski, V., Mehlig, M., and Filpula, D. (2003) Tailoring structure−function and pharmacokinetic properties of single-chain Fv proteins by site-specific PEGylation. *Protein Eng. 16*, 761−770.
(29) Lee, L. S., Conover, C., Shi, C., Whitlow, M., and Filpula, D. (1999) Prolonged circulating lives of single-chain Fv proteins conjugated with poly(ethylene glycol): a comparison of conjugation chemistries and compounds. *Bioconjugate Chem. 10*, 973−981.
(30) Greenwald, R. B., Yang, K., Zhao, H., Conover, C. D., Lee, S., and Filpula, D. (2003) Controlled release of proteins from their poly-(ethylene glycol) conjugates: drug delivery systems employing 1,6-elimination. *Bioconjugate Chem*. *14*, 395−403.
(31) Greenwald, R. B., Choe, Y. H., McGuire, J., and Conover, C. D. (2003) Effective drug delivery by PEGylated drug conjugates. *Adv. Drug Delivery Rev. 55*, 217−250.
(32) Greenwald, R. B., Zhao, H., Yang, K., Reddy, P., and Martinez, A. (2004) A new aliphatic amino prodrug system for the delivery of small molecules and proteins utilizing novel PEG derivatives. *J. Med. Chem. 47*, 726−734.
(33) Miron, T. and Wilchek, M. (1993) A simplified method for the preparation of succinimidyl carbonate poly(ethylene glycol) for coupling to proteins. *Bioconjugate Chem. 4*, 568−569.
(34) Roberts, M. J., Bentley, M. D., and Harris, J. M. (2002) Chemistry for peptide and protein PEGylation. *Adv. Drug Delivery Rev. 54*, 459−476.
(35) Martinez, A., Pendri, A., Xia, J. and Greenwald, R. B. (1997) Branched poly(ethylene glycol) linkers. *Macromol. Chem. Phys*. *198*, 2489−2498.
(36) Greenwald, R. B., Pendri, A., Martinez, A., Gilbert, C., and Bradley, P. (1996) PEG thiazolidine-2-thione, a novel reagent for facile protein modification: conjugation of bovine hemoglobin. *Bioconjugate Chem*. *7*, 638−641.
(37) Kinstler, O. B., Brems, D. N., Lauren, S. L., Paige, A. G., Hamburger, J. B., and Treuheit, M. J. (1996) Characterization and stability of N-terminally PEGylated rhG-CSF. *Pharm. Res*. *13*, 996−1002.
(38) Wang, M., Lee, L. S., Nepomich, A., Yang, J.-D., Conover, C., Whitlow, M. and Filpula, D. (1998) Single-chain Fv with manifold *N*-glycans as bifunctional scaffolds for immunomolecules. *Protein Eng*. *11*, 1277−1283.
(39) Harris, J. M. and Chess, R. B. (2003) Effect of PEGylation on pharmaceuticals. *Nat. Rev. Drug Discovery 2*, 214−221.
(40) Bailon, P., Palleroni, A., Schaffer, C. A., Spence, C. L., Fung, W. J., Porter, J. E., Ehrlich, G. K., Pan, W., Xu, Z. X., Modi, M. W., Farid, A., Berthold, W., and Graves, M. (2001) Rational design of a potent, long-lasting form of interferon: a 40 kDa branched polyethylene glycol-conjugated interferon α-2a for the treatment of hepatitis C. *Bioconjugate Chem. 12*, 195−202.
(41) Grace, M., Youngster, S., Gitlin, G., Sydor, W., Xie, L., Westreich, L., Jacobs, S., Brassard, D., Bausch, J., and Bordens, R. (2001) Structural and biologic characterization of pegylated recombinant IFN-α2b. *J. Interferon Cytokine Res. 21*, 1103−1115.
(42) Foser, S., Schacher, A., Weyer, K. A., Brugger, D., Dietel, E., Marti, S., and Schreitmuller, T. (2003) Isolation, structural characterization, and antiviral activity of positional isomers of monopegylated interferon α-2a (PEGASYS). *Protein Expr. Purif. 30*, 78−87.
(43) Rosendahl, M. S., Doherty, D. H., Smith, D. J., Carlson, S. J., Chlipala, E. A., and Cox, G. N. (2005) A long-acting, highly potent interferon α-2 conjugate created using site-specific PEGylation. *Bioconjugate Chem. 16*, 200−207.
(44) Peleg-Shulman, T., Tsubery, H., Mironchik, M., Fridkin, M., Schreiber, G., and Shechter, Y. (2004) Reversible PEGylation: a novel technology to release native interferon α2 over a prolonged time period. *J. Med. Chem*. *47*, 4897−4904.
(45) Wang, Y.-S., Youngster, S., Grace, M., Bausch, J., Bordens, R. And Wyss, D. F. (2002) Structural and biological characterization of pegylated recombinant interferon alpha-2b and its therapeutic implications. *Adv. Drug Delivery Rev. 54*, 547−570.
(46) Pepinsky, R. B., Lepage, D. J., Gill, A., Chakraborty, A., Vaidyanathan, S., Green, M., Baker, D. P., Whalley, E., Hochman, P. S., and Martin, P. (2001) Improved pharmacokinetic properties of a polyethylene glycol-modified form of interferon-β-1a with preserved *in vitro* bioactivity. *J. Pharmacol. Exp. Ther. 297*, 1059−1066.
(47) Mager, D. E., Neuteboom, B., and Jusko, W. J. (2005) Pharmacokinetics and pharmacodynamics of PEGylated IFN-β 1a following subcutaneous administration in monkeys. *Pharm. Res. 22*, 58−61.

(48) Katre, N. and Knauf, M. J. (1990) Solubilization of immunotoxins for pharmaceutical compositions using polymer conjugation. U. S. Patent Number 4,917, 888.

(49) Chapman, A. P. (2002) PEGylated antibodies and antibody fragments for improved therapy: a review. *Adv. Drug Delivery Rev. 54*, 531−545.

(50) Clark, R., Olson, K., Fuh, G., Marian, M., Mortensen, D., Teshima, G., Chang, S., Chu, H., Mukku, V., Canova-Davis, E., Somers, T., Cronin, M., Winkler, M., and Wells, J. A. (1996) Long-acting growth hormones produced by conjugation with poly(ethylene glycol). *J. Biol. Chem. 271*, 21969−21977.

(51) Pettit, D. K., Bonnert, T. P., Eisenman, J., Srinivasan, S., Paxton, R., Beers, C., Lynch, D., Miller, B., Yost, J., Grabstein, K. H., and Gombotz, W. R. (1997) Structure−function studies of interleukin 15 using site-specific mutagenesis, poly(ethylene glycol) conjugation, and homology modeling. *J. Biol. Chem. 272*, 2312−2318.

(52) Yamamoto, Y., Tsutsumi, Y., Yoshioka, Y., Nishibata, T., Kobayashi, K., Okamoto, T., Mukai, Y., Shimizu, T., Nakagawa, S., Nagata, S., and Mayumi, T. (2003) Site-specific PEGylation of a lysine-deficient TNF-α with full bioactivity. *Nat. Biotechnol. 21*, 546−552.

(53) Walter, M. R., Windsor, W. T., Nagabhushan, T. L., Lundell, D. J., Lunn, C. A., Zauodny, P. J., and Narula, S. K. (1995) Crystal structure of a complex between interferon-γ and its soluble high-affinity receptor. *Nature 37*, 230−235.

(54) Lin, L. S., Yamamoto, R. and Drummond, R. J. (1986) Purification of recombinant human interferon beta expressed in *Escherichia coli*. *Methods Enzymol. 119*, 183−192.

(55) Russell-Harde, D., Knauf, M., and Croze, E. (1995) The use of zwittergent 3−14 in the purification of recombinant human interferon-β ser^{17} (Betaseron). *J. Interferon Cytokine Res. 15*, 31−37.

(56) Smith, P. K., Krohn, R. I., Hermanson, G. T., Mallia, A. K., Gartner, F. H., Provenzano, M. D., Fujimoto, E. K., Goeke, N. M., Olson, B. J. and Klenk, D. C. (1985) Measurement of protein using bicinchoninic acid. *Anal. Biochem. 150*, 76−85.

(57) Carrey, E. A. (1989) Peptide mapping. In *Protein Structure: A Practical Approach* (Creighton, T. E., Ed.) pp 117−144, Oxford University Press, Oxford.

(58) Greenfield, N. J., Montelione, G. T., Farid, R. S., and Hitchcock-DeGregori, S. E. (1998) The structure of the N-terminus of striated muscle alpha-tropomyosin in a chimeric peptide: nuclear magnetic resonance structure and circular dichroism studies. *Biochemistry 37*, 7834−7843.

(59) Bohm, G., Muhr, R., and Jaenicke, R. (1992) Quantitative analysis of protein far UV circular dichroism spectra by neural networks. *Protein Eng. 5*, 191−195.

(60) Familletti, P. C., Rubinstein, S. and Pestka, S. (1981) A convenient and rapid cytopathic effect inhibition assay for interferon. *Methods Enzymol. 78*, 387−394.

(61) Garrison, T. L., Hung, F., Izotova, L., Schwartz, B., Lavoie, T. and Lee-Own, F. V. (2002) ELISA measurement of interferons. *Biotechniques 33*, S98−S100.

BC050322Y